

Pionic hydrogen and deuterium

D. Gotta^{1,*}, F. D. Amaro², D. F. Anagnostopoulos³, P. Bühler⁴, D. S. Covita^{2,5}, H. Fuhrmann⁴, H. Gorke⁶, A. Gruber⁴, M. Hennebach¹, A. Hirtl⁴, T. Ishiwatari⁴, P. Indelicato⁷, T. S. Jensen^{5,8}, E.-O. Le Bigot⁷, Y.-W. Liu⁵, B. Manil⁷, V. E. Markushin⁵, J. Marton⁴, M. Nekipelov¹, V. N. Pomerantsev⁹, V. P. Popov⁹, A. J. Rusi el Hassani¹⁰, J. M. F. dos Santos², S. Schlessler⁷, Ph. Schmid⁴, L. M. Simons⁵, Th. Strauch¹, M. Theisen¹, M. Trassinelli¹¹, J. F. C. A. Veloso¹², and J. Zmeskal⁴

¹Institut für Kernphysik, Forschungszentrum Jülich, 52425 Jülich, Germany

²LIBPhys, Physics Department, Coimbra University, 3004-526 Coimbra, Portugal

³Dept. of Materials Sci. and Eng., University of Ioannina, Ioannina, 45110, Greece

⁴Stefan Meyer Institute for Subatomic Physics, Austrian Academy of Sciences, 1030 Vienna, Austria

⁵Laboratory for Particle Physics, Paul Scherrer Institute, 5232 Villigen, Switzerland

⁶Zentralinstitut für Elektronik, Forschungszentrum Jülich, 52425 Jülich, Germany

⁷LKB, Sorbonne Université, CNRS, ENS-PSL, Collège de France, 4 place Jussieu, 75005 Paris, France

⁸Institut für Theoretische Physik Universität Zürich, 8057 Zürich, Switzerland

⁹Skobeltsyn Inst. of Nuclear Physics, Lomonosov Moscow State University, 119234 Moscow, Russia

¹⁰Faculté des Sciences et Techniques, Université Abdelmalek Essaâdi, Tanger, Morocco

¹¹Institut des NanoSciences de Paris, CNRS, Sorbonne Université, 4 place Jussieu, 75005 Paris, France

¹²IZN, Dept. of Physics, Aveiro University, 3810 Aveiro, Portugal

Abstract. The strong-interaction effects both in pionic hydrogen and deuterium atoms have been re-determined with improved precision. The hadronic shift and width in pionic hydrogen together with the hadronic shift in pionic deuterium constitute a one-fold constraint for the two independent pion-nucleon scattering lengths. Furthermore, the hadronic width in pionic deuterium measures the transition strength of s-wave pions on an isoscalar nucleon-nucleon pair which is an independent quantity not related to the pion-nucleon scattering lengths. The experiment was performed at the Paul Scherrer Institute by stopping a high-intensity low-energy pion beam in gaseous targets using the cyclotron trap. The X-rays emitted by the πH and πD atoms were analysed with a high resolution Bragg spectrometer equipped with spherically bent crystals. The pion-nucleon scattering lengths and other physical quantities extracted from the atom data are in good agreement with the results obtained from pion-nucleon and nucleon-nucleon scattering experiments and confirm that a consistent picture is achieved for the low-energy pion-nucleon sector with respect to the expectations of chiral perturbation theory.

1 Introduction

The pion-nucleon (πN) interaction at low energies plays a prominent role in the understanding of the strong interaction. Hence, $\pi N \rightarrow \pi N$ reactions and the corresponding scattering

*e-mail: d.gotta@fz-juelich.de

lengths are of fundamental interest. Therefore, a comparison of the results from precision experiments with advanced theoretical calculations is of great importance. The calculations have been performed in the frame work of effective field theories like Chiral Perturbation theory (χ PT), which predict isospin-breaking effects to be of the order of a few per cent.

The experimental approach is achieved by means of high-resolution X-ray spectroscopy of pionic hydrogen and deuterium atoms. Such atomic systems are formed when pions are decelerated to kinetic energies corresponding to bound states in the Coulomb potential of a nucleus. After capture, pions undergo an atomic de-excitation cascade, where in the last steps emission of characteristic X-rays occurs. In the case of pionic hydrogen and deuterium, the strong-interaction manifests as an energy shift ϵ_{1s} and broadening Γ_{1s} of the atomic ground state $1s$ (fig. 1). Considering the energy regime of the atomic systems, the measurement of ϵ_{1s} and Γ_{1s} constitutes a scattering experiment at threshold.

The hadronic effects are related in leading order to specific πN reactions. Where $\epsilon_{1s}^{\pi H}$ is attributed to elastic scattering $\pi^- p \rightarrow \pi^- p$, $\Gamma_{1s}^{\pi H}$ is due to charge exchange $\pi^- n \rightarrow \pi^0 n$. For $\epsilon_{1s}^{\pi D}$, it is the coherent sum of $\pi^- p \rightarrow \pi^- p$ and $\pi^- n \rightarrow \pi^- n$ where, however, substantial corrections because of 3-body effects must be taken into account.

In the limit of isospin conservation, all $\pi N \rightarrow \pi N$ reactions are completely determined by only two independent real numbers, the scattering lengths corresponding to the isospin combinations $I = 1/2$ and $3/2$ of the πN system. In the isospin basis, the scattering lengths of the reaction channels read $a_{\pi^- p \rightarrow \pi^- p} = \frac{1}{3}(2a_{1/2} + a_{3/2})$, $a_{\pi^- p \rightarrow \pi^0 n} = -\frac{\sqrt{2}}{3}(a_{1/2} - a_{3/2})$, and $a_{\pi^+ p \rightarrow \pi^+ p} = a_{\pi^- n \rightarrow \pi^- n} = a_{3/2}$ leading to the so-called isospin triangle relation $a_{\pi^- p \rightarrow \pi^- p} - a_{\pi^+ p \rightarrow \pi^+ p} = -\sqrt{2}a_{\pi^- p \rightarrow \pi^0 n}$. It is convenient to use also as the two independent quantities the isoscalar and isovector scattering lengths given by $a^\pm \equiv (a_{\pi^- p \rightarrow \pi^- p} \pm a_{\pi^+ p \rightarrow \pi^+ p})$. The relations of the various scattering lengths to $\epsilon_{1s}^{\pi H}$, $\Gamma_{1s}^{\pi H}$, and $\epsilon_{1s}^{\pi D}$ are indicated in table 1.

In contrast hereto, $\Gamma_{1s}^{\pi D}$ is not due to scattering but to true pion absorption $\pi NN \rightarrow NN$ by an $I = 0$ nucleon-nucleon pair. Considering charge symmetry ($\pi^- d \rightarrow nn \Leftrightarrow \pi^+ d \rightarrow pp$) and detailed balance ($\pi^+ d \rightarrow pp \Leftrightarrow pp \rightarrow \pi^+ d$), except for small isospin-breaking corrections, all three reactions are described by the same transition matrix elements. Hence, the hadronic width in πD directly yields the pion-production transition strength at threshold, denoted α , when corrected for the radiative capture channels $\pi NN \rightarrow NN\gamma$ (tab. 1).

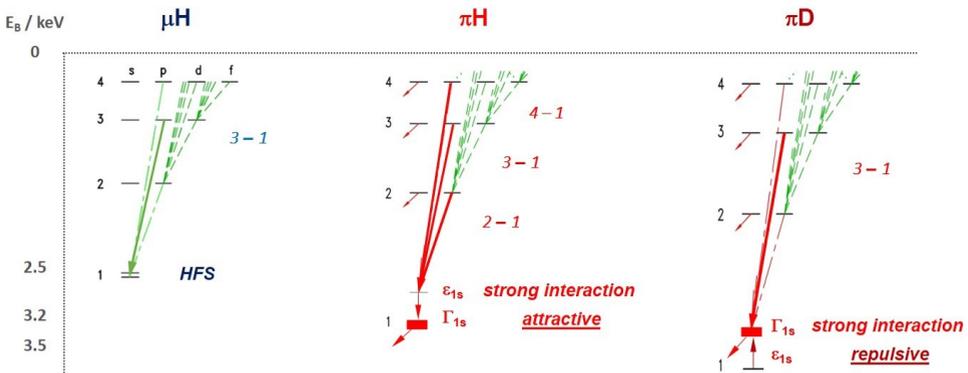


Figure 1. Scheme of low-lying atomic levels of muonic (μH) and pionic hydrogen (πH) and pionic deuterium (πD). Lyman transitions ($n - 1$) measured in this experiment are indicated. The sign convention for the hadronic shift is $\epsilon \equiv E_X - E_{QED}$, which corresponds to the change of the X-ray transition energy E_X compared to the pure electromagnetic value E_{QED} .

This paper recapitulates the final results of a long series of experiments [1] aiming at the improved determination of the strong-interaction effects both in pionic hydrogen and deuterium [2–8]. Concepts and recent theoretical efforts on low-energy πN scattering and pionic hydrogen are reviewed in [9, 10]. Properties of low Z exotic atoms, experimental methods, and the performance of the crystal spectrometer are outlined in [11, 12].

2 Experiment

In the case of muonic and pionic hydrogen, only X-rays from the K series (fig.2 - left) are accessible within this experimental scheme (fig.4). High resolution and high statistics measurements are confronted with various physical effects during the de-excitation cascade and need highly advanced experimental methods.

2.1 Cascade effects

The upper part of the atomic cascade is dominated by non-radiative de-excitation collision-induced reactions. Three different reactions must be considered in particular. At first, Stark mixing leads to mixing of the angular momentum states when the exotic hydrogen atom penetrates the Coulomb field of H atoms of the H_2 molecules in the target [13]. The resulting s -state admixture in the high-lying levels leads for pions to a significant reduction of X-ray line yields because of nuclear reactions (fig. 2 - right).

Secondly, additional X-ray energy shifts, thus falsifying the result for the strong-interaction shift ϵ , may occur due to molecular formation $\pi^-H+H_2 \rightarrow [(\pi^-pp) \cdot p]ee$ if radiative de-excitation from molecular levels exists [14, 15].

Coulomb de-excitation is a non-radiative de-excitation step ($n - n'$), where the energy is transferred into kinetic energy of the collision partners [19]. The competition of acceleration by Coulomb de-excitation and deceleration by elastic and inelastic collisions leads to a complex kinetic energy distribution at the time of X-ray emission. Advanced models like the extended standard cascade model (ESCM) follow the development of the kinetic energy distribution during de-excitation [20–23] (fig. 3 - left) which in turn required an update of the corresponding collision cross sections [24–26]. The resulting Doppler broadening can be demonstrated clearly in the line shape of the $\mu H(3p - 1s)$ line (fig. 3 - right). The correction

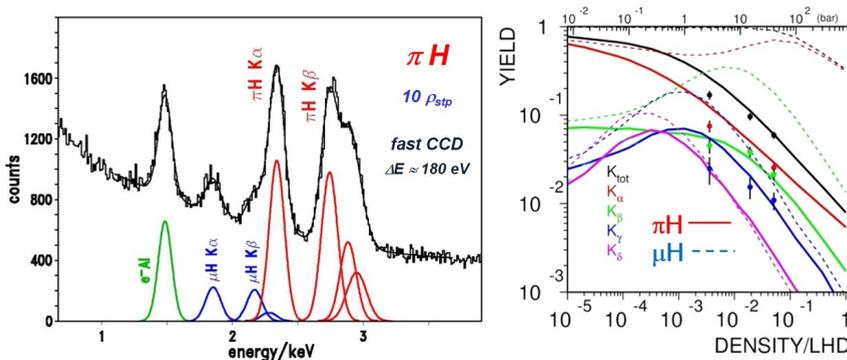


Figure 2. Left: K series of pionic hydrogen measured with a fast read-out pnCCD [16]. Muonic X-rays stem from decay muons stopped in H_2 target. Right: K yields in pionic and muonic hydrogen as calculated with the ESCM cascade model [17]. The data points are from [18].

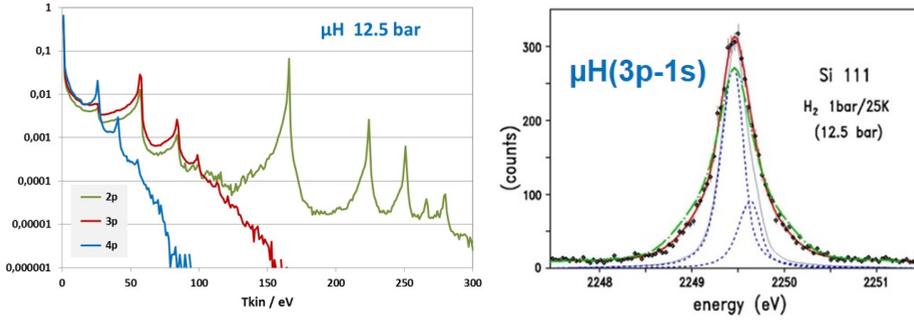


Figure 3. Left: theoretical prediction for the kinetic energy spectrum at the time of the emission of the $\mu\text{H}(3p-1s)$ transition. Right: measured line shape of the $\mu\text{H}(3p-1s)$ transition using the silicon 111 reflection. The narrow structures inside the μH line display the two hyperfine transitions as given by the spectrometer resolution only [7].

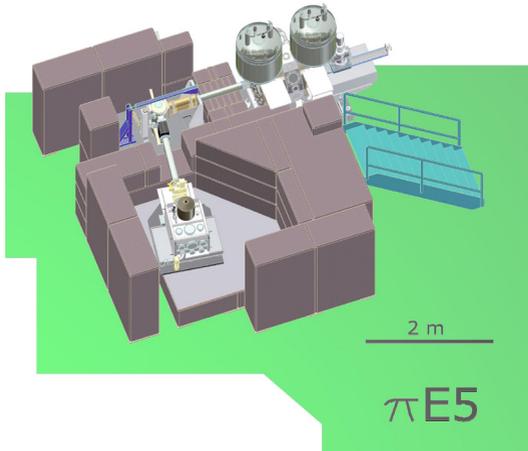


Figure 4. Set-up in the πE5 area at PSI for the $\pi\text{H}(4-1)$ [2] and the $\pi\text{D}(3-1)$ line [5]. The Bragg crystal is mounted inside a vacuum chamber (upper left) and connected to the cyclotron trap (upper right) and the CCD X-ray detector (lower left) by a vacuum system to minimize absorption losses. Bragg angles for the Si 111 reflection are $\Theta_B = 40.5^\circ$ and 40.0° , respectively. The roof of the concrete shielding is not shown.

for the Doppler broadening is essential for a precise determination of the strong-interaction broadening Γ .

2.2 Set-up

The energy shift ϵ_{1s} is of the order of a few eV and the broadening $\Gamma_{1s} \approx 1$ eV, whereas the $(np-1s)$ X-ray energies are around 3 keV (fig. 2 - left). The precise measurement of such a small line broadening requires high-resolution devices like crystal spectrometers, which in turn need strong X-ray sources. For this reason, precision results were not attainable before high-intensity and low-energy pion beams became available.

In order to improve the quality of the results for the strong-interaction effects compared to previous experiments [27–31], a specifically developed cyclotron trap [32] was used together with a Johann-type spectrometer equipped with spherically bent Bragg crystals as well as a large area array of charge-coupled devices (CCDs) [33]. The experiment benefited from a 4-fold higher beam intensity provided at the Paul Scherrer Institute (Villigen, Switzerland). Statistics and peak-to-background ratio were improved by a factor of about 30 and 50 by setting up a massive specially tailored concrete shielding, respectively.

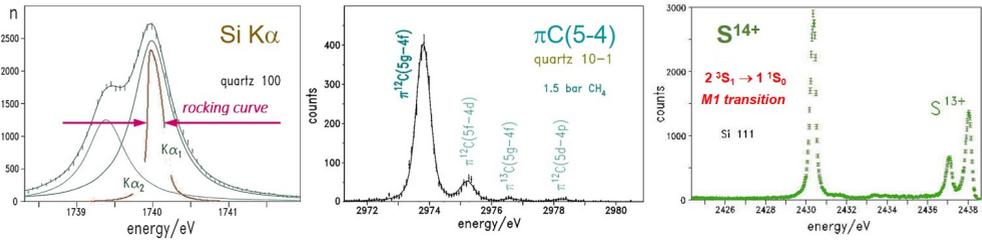


Figure 5. Left: medium Z fluorescence X-ray widths exceed the crystal resolution (rocking curve width) due to the large Auger width. Middle: pionic atoms measurements provide narrow X-ray lines but suffer from too low statistics for systematic crystal studies. Right: up to 10000 events per hour have been recorded in M1 transitions of He-like medium Z atoms [34].

Only silicon and quartz crystals meet the requirements for the resolutions needed. Thin polished slabs were spherically bent to radii of about $R_c = 3$ m by attaching them to glass lenses of optical quality by adhesive forces only. Resolutions of 270 – 460 meV, which are close to the theoretical limit, were achieved for the X-rays in the energy range of 2.2–3.1 keV.

The main obstacle to a precision determination of the hadronic broadening Γ_{1s} is Doppler broadening due to Coulomb de-excitation. Consequently, the ultimate knowledge of the spectrometer response function is of great importance and conventional methods to determine it are marginal (fig. 5 - left and middle).

Here, the cyclotron trap offers the unique possibility for a new calibration method when extended to operate as ECR source [35]. The ECR source yields narrow X-rays at high rates from helium-like low Z elements like sulphur, chlorine, and argon which almost coincide in energy with the pionic hydrogen and deuterium X-ray transitions (fig. 5 - right).

The kinetic energy distribution of the π H atoms develops during the atomic cascade and, in addition as a collision-induced process, must be assumed to be density dependent. As a result, the influence of the Doppler effect depends on the initial state np and the target density. Also, the molecular formation rate scales with collision probability. A density dependence of X-ray energies would demonstrate the appearance of X-ray emission from molecular states.

Therefore, three different ground-state transitions, π H($2p - 1s$), π H($3p - 1s$), and π H($4p - 1s$) ($K\alpha$, $K\beta$, and $K\gamma$), have been measured at hydrogen densities between 3.9 bar and liquid (LH_2). Furthermore, the measured line shape is a convolution of spectrometer response, Doppler broadening, and the Lorentzian representing the hadronic broadening. For that reason, the measurement of the twin system μ H offered the chance to study the Doppler broadening without the hadronic contribution to the line width (fig. 3 - right).

3 Analysis

3.1 Hadronic shift

The Johann-type set-up of the crystal spectrometer requires a calibration line, preferentially as close as possible in the Bragg angle of the corresponding π H line [12, 36]. For the π H($3p - 1s$) transition, the energy of the π O($6h - 5g$) line almost coincides (fig. 6). This line provides a superior calibration standard compared to the fluorescence X-rays, because π O($6h - 5g$) X-rays originate from hydrogen-like pionic atoms, the energy levels of which can be calculated to ± 7 meV, where about ± 6 meV are due to the uncertainty of the pion mass. No change of the set-up is required between measurement and calibration except a gas exchange in the

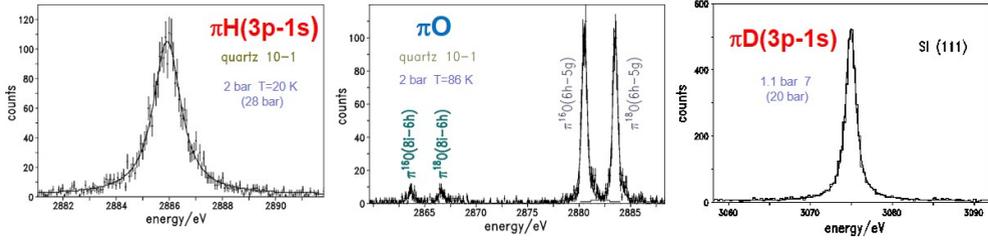


Figure 6. The energy calibration for the $\pi\text{H}(3p - 1s)$ measurements were performed with X-rays from fully stripped pionic oxygen using the $\pi\text{O}(6h - 5g)$ line [2]. For the $\pi\text{D}(3p - 1s)$ line, Ga $K\alpha$ fluorescence X-rays measured in 3rd order served as energy calibration [5].

target cell. At the lowest density, by using an O_2/H_2 gas mixture, both lines can be measured simultaneously.

For the $\pi\text{H}(2p - 1s)$, $\pi\text{H}(4p - 1s)$, and $\pi\text{D}(3p - 1s)$ transitions measured in this experiment series [2, 5], fluorescence X-rays served as calibration standard as in previous experiments [27–31]. Results for $\epsilon_{1s}^{\pi\text{H}}$ are in perfect agreement with the ones using the πO calibration. The uncertainties of the energies of fluorescence X-rays, however, amount to $\pm(27 - 73)$ meV for the cases considered here.

No density dependence of X-ray energies was observed for either hydrogen and deuterium, *i. e.* X-ray emission from molecular orbits does not play any role for the accuracy of the data given [2, 5].

Worthwhile to mention, that a discrepancy for $\epsilon_{1s}^{\pi\text{H}}$ between the new result [2] and previous experiments disappears when readjusting the older values with a new calculation of the pure electromagnetic transition energy [37].

3.2 Hadronic broadening

The analysis of the μH , πH , and πD line shapes uses a model for the kinetic energy distribution which reduces its complexity to a few prominent components [4–8]. The model distribution consists always of a low-energy part which takes into account non accelerated or already again decelerated atoms. Depending on the initial level of the X-ray emission, up to three high-energy components were considered with the energies inspired by the fact that a few dominant Coulomb transitions dominate the Doppler broadening.

The model line profiles $LP = R \otimes L \otimes (\sum_i D_i)$ are build up by the convolution of the spectrometer response R , the natural line with L which corresponds to Γ_{1s} , and the components $(\sum_i D_i)$ modelling the kinetic energy distribution.

Both a χ^2 (frequentist) analysis and a Bayesian analysis were performed for pionic and muonic hydrogen. The non-trivial model parameters of the analyses were Γ_{1s} , the relative intensities of the Doppler components D_i , and the energies of the high-energetic components.

The use of a Bayesian approach for πH and μH was motivated by the case of pionic deuterium. There, the occurrence of a bias in a frequentist method [38], influencing the extracted values for $\Gamma_{1s}^{\pi\text{D}}$, has been studied in detail [5]. Such a bias stems from the — principally unknown — difference of the probability distribution of the data itself and the one assumed for the model. An estimate for the bias of the parameter $\Gamma_{1s}^{\pi\text{D}}$ was obtained by performing with the model as used in the analysis a series of Monte-Carlo simulations to generate the X-ray line shape and, after analysis, comparing input and output parameters. This lengthy procedure may be circumvented by using Bayesian methods, which are supposed to be free from bias

effects in parameter estimation [39]. Furthermore, comparing the results of the two analysis methods establishes an independent consistency check.

Both the frequentist as well as the Bayesian analyses clearly show that a distinctive low-energy component of the kinetic energy distribution exists containing about 2/3 of the total intensity. As expected, it is impossible to resolve the complex structure of the kinetic energy spectrum at higher energies in the presence of a hadronic broadening with the data given. However, it can be effectively modelled by one or two high-energy components and the details of these components are not critical for the numerical result of $\Gamma_{1s}^{\pi H}$ but limits the accuracy to about 3%. To summarize the current situation one can assert that the theoretical prediction for the kinetic energy distributions and the experimental results do not show any drastic inconsistencies. The weighted average for the strong-interaction effects over the various transitions and target densities measured is given in table 1.

It is worth mentioning that in pionic deuterium no Doppler broadening due to Coulomb de-excitation could be identified within the experimental uncertainties [5]. A theoretical explanation for such behaviour has been provided recently by cascade theory [40].

Table 1. Results for the strong-interaction effects ϵ_{1s} and Γ_{1s} in pionic hydrogen and deuterium (in meV) and their relation to πN scattering and absorption reactions as well as to the isoscalar and isovector scattering length a^+ and a^- and the threshold pion production strength α .

$\epsilon_{1s}^{\pi H}$	$\Gamma_{1s}^{\pi H}$	$\epsilon_{1s}^{\pi D}$	$\Gamma_{1s}^{\pi D}$
7085.8 ± 9.6 [2]	856 ± 27 [8]	-2356 ± 31 [5]	1171^{+23}_{-49} [5]
$\pi^- p \rightarrow \pi^- p$	$\pi^- p \rightarrow \pi^0 n$	$\pi^- p \rightarrow \pi^- p + \pi^- n$	$\Gamma_{\pi^- d \rightarrow nn+\pi\gamma}$
$\propto (a^+ + a^-) + \dots$	$\propto (a^-)^2 + \dots$	$\propto 2a^+ + \dots$	α

3.3 Results

The three independent experimental results for the strong-interaction shifts in πH and πD together with the hadronic broadening in πH yield a onefold constraint for any combination of the two independent πN scattering length. As shown in fig. 7 - left, a consistent picture is achieved by applying the corrections as worked out in the framework of χPT [10, 41, 42]. The uncertainty for the scattering lengths as determined from the two shifts is mainly attributed to the poor knowledge of LECs, whereas in the case of the hadronic broadening the experimental error is about twice the one of the chiral corrections.

In addition to the scattering length of the reactions $\pi^- p \rightarrow \pi^- p$ and $\pi^- n \rightarrow \pi^0 n$, the scattering length for the reaction $\pi^+ p \rightarrow \pi^+ p$ is accessible via the triangle relation applying appropriate chiral corrections. Furthermore, the πN coupling constant $g_c^2/4\pi$ [43], the pion photo-production strength at threshold $E_{0^+}^{thr}$ [44], or the πN σ -term $\sigma_{\pi N}$ [45] also are related to the isoscalar and isovector scattering lengths. A comparison of the these quantities derived from pionic-atom data and other sources is shown in fig. 8. In general, data from various sources are highly consistent when analysed within the framework of χPT [42, 46, 47]. For $\sigma_{\pi N}$, a discrepancy of about 20 MeV remains between the experiment based values [8, 47–49] and lattice calculations [50–53] which, however, may be removed by including $N\pi$ and $N\pi\pi$ contributions [54].

The result for the pion-production strength α , extracted from the strong-interaction width in πD , is compared to the results from pion-production experiments in fig. 7 - right. The theoretical approach within the frame work of χPT suffers again from the scarce precision of some LECs [57].

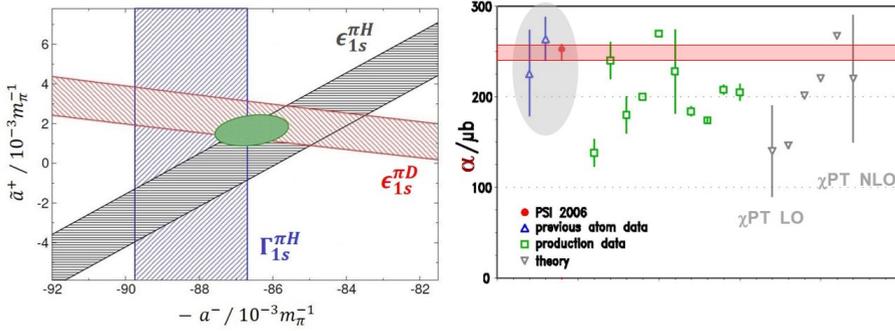


Figure 7. Left: constraints (bands) and combined result (ellipse) for the isoscalar and isovector πN scattering lengths \tilde{a}^+ and a^- as derived from $\epsilon_{1s}^{\pi H}$, $\epsilon_{1s}^{\pi D}$, and $\Gamma_{1s}^{\pi H}$ [8]. Right: comparison of results for pion-production strength α at threshold on isoscalar NN pairs. The horizontal band represents the precision of the most recent result for $\Gamma_{1s}^{\pi D}$ [5].

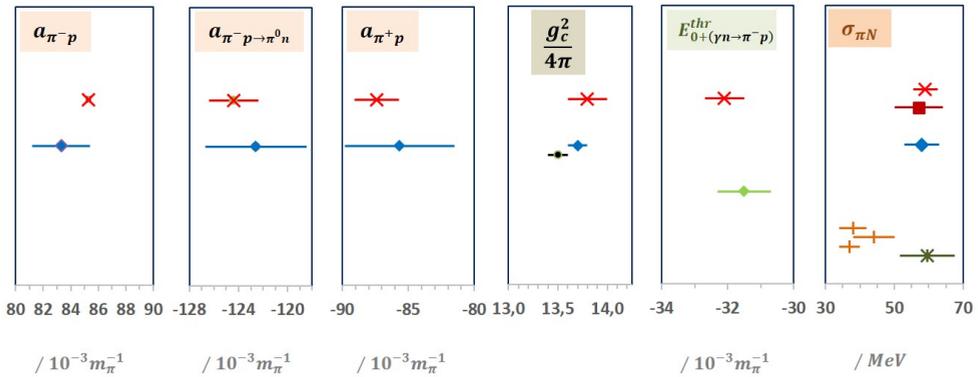


Figure 8. Comparison of parameters derived from pionic hydrogen and deuterium strong-interaction effects $\epsilon_{1s}^{\pi H}$, $\epsilon_{1s}^{\pi D}$, and $\Gamma_{1s}^{\pi H}$ (\times [2, 3, 5, 8]) and results from other sources (\blacksquare higher Z pionic-atoms in medium fit [49], \blacklozenge πN scattering analysis based on Roy-Steiner equations [48], \bullet NN scattering [55], \blacktriangle Photo production [56], $+$ lattice calculations [50–53], \ast lattice calculations including low-lying $N\pi$ and $N\pi\pi$ states [54]).

3.4 Conclusion and outlook

In summary, recent πH , πD , and low-energy πN scattering data are quantitatively consistent when analysed within the framework of χ PT. In view of the difficulties arising from the line-shape corrections due to Coulomb de-excitation, future experiments should preferably use X-ray transitions from higher np initial states where the Doppler broadening is expected to be smaller. Since the accelerator currents improve continuously with time, measurements with sufficient statistics for the $(4 - 1)$ or even $(5 - 1)$ transition will become feasible. In this respect it is important to emphasize that the coverage of a sufficiently large energy interval around the transition is essential to fix the background level on both sides of the line. In this way, an accuracy of 1% or better can be achieved for the hadronic width of pionic hydrogen.

References

- [1] PSI proposals R-98.01 and R-06.03, <http://collaborations.fz-juelich.de/ikp/exotic-atoms>
- [2] M. Hennebach et al., *Eur. Phys. J. A* **50**, 190 (2014)
- [3] M. Hennebach et al., *Eur. Phys. J. A* **55**, 24(E) (2019)
- [4] T. Strauch et al., *Phys. Rev. Lett.* **104**, 142503 (2010)
- [5] T. Strauch et al., *Eur. Phys. J. A* **47**, 88 (2011)
- [6] D.S. Covita et al., *Phys. Rev. Lett.* **102**, 023401 (2009)
- [7] D.S. Covita et al., *Eur. Phys. J. D* **72**, 72 (2018)
- [8] A. Hirtil et al., *Eur. Phys. J. A* **57**, 70 (2021)
- [9] J. Gasser, V.E. Lyubovitzkij, A. Rusetski, *Phys. Rep.* **456**, 167 (2008)
- [10] M. Hoferichter et al., *Phys. Rep.* **625**, 1 (2016)
- [11] D. Gotta, *Prog. Part. Nucl. Phys* **52**, 133 (2004)
- [12] D.E. Gotta, L.M. Simons, *Spectrochim. Acta B* **120**, 9 (2016)
- [13] M. Leon, H. Bethe, *Phys. Rev.* **127**, 636 (1962)
- [14] S. Jonsell, J. Wallenius, P. Froelich, *Phys. Rev. A* **59**, 3440 (1999)
- [15] S. Kilic, J.P. Karr, L. Hilico, *Phys. Rev. A* **70**, 042506 (2004)
- [16] H. Gorke et al., *AIP Conf. Proc.* **793**, 341 (2005)
- [17] T.S. Jensen, V.E. Markushin, *Hyperfine Int.* **138**, 71 (2001)
- [18] A.J. Rusi el Hassani et al., *Z. Phys. A* **351**, 113 (1995)
- [19] L. Bracchi, G. Fiorentini, *Nuovo Cim. A* **43**, 9 (1978)
- [20] V.E. Markushin, *Phys. Rev A* **50**, 1137 (1994)
- [21] T.S. Jensen, V.E. Markushin, *Lec. Notes Phys.* **627**, 37 (2003)
- [22] T.S. Jensen, V.P. Popov, V.N. Pomerantsev, arXiv:0712.3010 [nucl-th] (2007)
- [23] V.P. Popov, V.N. Pomerantsev, *Hyperfine Int.* **209**, 75 (2012)
- [24] T.S. Jensen, V.E. Markushin, *Eur. Phys. J. D* **21**, 165 (2002)
- [25] V.N. Pomerantsev, V.P. Popov, *Phys. Rev. A* **73**, 040501(R) (2006)
- [26] V.P. Popov, V.N. Pomerantsev, *Phys. Rev. A* **86**, 052520 (2012)
- [27] D. Sigg et al., *Phys. Rev. Lett.* **75**, 3245 (1995)
- [28] D. Sigg et al., *Nucl. Phys. A* **609**, 269 (1996)
- [29] D. Sigg et al., *Nucl. Phys. A* **617**, 526 (1997)
- [30] H.C. Schröder et al., *Phys. Lett. B* **469**, 25 (1999)
- [31] H.C. Schröder et al., *Eur. Phys. J. C* **21**, 473 (2001)
- [32] D. Gotta, L.M. Simons, *SciPost Phys. Proc.* **5**, 013 (2021)
- [33] N. Nelms et al., *Nucl. Instr. Meth. A* **484**, 419 (2002)
- [34] D.F. Anagnostopoulos et al., *Nucl. Instr. and Meth. A* **545**, 217 (2005)
- [35] S. Biri, L. Simons, D. Hitz, *Rev. Sci. Instrum.* **71**, 1116 (2000)
- [36] M. Trassinelli et al., *Phys. Lett. B* **759**, 583 (2016)
- [37] S. Schlessler et al., *Phys. Rev. C* **84**, 015211 (2011)
- [38] U.C. Bergmann, K. Riisager, *Nucl. Instr. Methods A* **489**, 444 (2002)
- [39] R.D. Cousins, *Am. J. Phys.* **63**, 398 (1995)
- [40] V.P. Popov, V.N. Pomerantsev, *Phys. Rev. A* **95**, 022506 (2017)
- [41] V. Baru et al., *Nucl. Phys. A* **872**, 69 (2011)
- [42] V. Baru et al., *Phys. Lett. B* **694**, 473 (2011)
- [43] M.L. Goldberger, H. Miyazawa, R. Oehme, *Phys. Rev.* **99**, 986 (1955)
- [44] N.M. Kroll, M.A. Ruderman, *Phys. Rev.* **93**, 233 (1954)

- [45] J. Gasser, H. Leutwyler, M.E. Sainio, Phys. Lett. B **253**, 252 (1991)
- [46] V. Bernard, N. Kaiser, U.G. Meißner, Phys. Lett. B **383**, 116 (1996)
- [47] M. Hoferichter, J. Ruiz de Elvira, B. Kubis, U.G. Meißner, Phys. Rev. Lett. **115**, 092301 (2015)
- [48] J. Ruiz de Elvira et al., J. Phys. G **45**, 024001 (2018)
- [49] E. Friedman, A. Gal, Phys. Lett. B **792**, 340 (2019)
- [50] S. Dürr et al., Phys. Rev. Lett. **116**, 172001 (2016)
- [51] S. Dürr et al., Phys. Rev. Lett. **116**, 172001 (2016)
- [52] A. Abdel-Rehim et al., Phys. Rev. Lett. **116**, 252001 (2016)
- [53] S. Borsanyi et al., arXiv:2007.03319v1 [hep-lat] (2020)
- [54] R. Gupta et al., Phys. Rev. Lett. **127**, 242002 (2021)
- [55] M.C.M. deSwart, J. J. and Rentmeester, R.G.E. Timmermans, PiN Newsl. **13**, 96 (1997)
- [56] M.A. Kovash, PiN Newsl. **12**, 51 (1997)
- [57] V. Lensky et al., Eur. Phys. J. A **27**, 37 (2006)